

Competitive Orders in Altermagnetic Chiral Magnons

Congzhe Yan¹ and Jinyang Ni^{2,*}

¹Department of Physics, University of Science and Technology of China, Hefei, Anhui, 230026, China

²Ministry of Education Key Laboratory for Nonequilibrium Synthesis and Modulation of Condensed Matter, Shaanxi Province Key Laboratory of Advanced Functional Materials and Mesoscopic Physics, School of Physics, Xi'an Jiaotong University, Xi'an 710049, China

(Dated: November 7, 2025)

In altermagnets, magnons—the quanta of collective spin excitations—exhibit chiral splitting even in the absence of spin-orbit coupling and external magnetic fields. Typically, this chiral splitting behavior can be well described by alternating isotropic spin exchanges (ISE) in the low-temperature regime; however, its dynamic behavior at a finite temperature remains unclear. In this study, we reveal that, when including magnon–magnon interactions, long-range anisotropic spin exchange (ASE) can also induce chiral splitting of magnons at a finite temperature. Crucially, the chiral splitting induced by ASE competes with that arising from ISE, leading to a pronounced temperature-dependent modulation of the altermagnetic chiral splitting. Moreover, this competition is intimately connected to spin fluctuations, and can reverse the spin current driven by the band splitting as temperature increases. Our work uncovers the intrinsic competition governing collective spin excitations in altermagnets, providing new insights into their finite-temperature dynamical behavior.

Introduction. Conventional collinear antiferromagnets exhibit zero net magnetization and are preserved under translation (τ) and inversion (\mathcal{P}) symmetry, resulting in spin-degenerate bands [1, 2]. However, recent studies have shown that when opposite-spin sublattices are no longer linked by translation or inversion symmetry but instead by additional rotational or mirror symmetry operations [3, 4], such magnetic states can exhibit momentum-dependent spin-split bands even in the absence of spin-orbit coupling (SOC). This phenomenon has been experimentally confirmed in candidate materials, dubbed as altermagnets [5–12]. For example, in a d -wave altermagnet on a square lattice, the sublattices are related by a spin flip combined with a $\pi/2$ real-space rotation about a point on the dual lattice, as illustrated in Fig. 1. The ability to combine ferromagnetic-like spin splitting with zero net magnetization avoids adverse stray-field effects during ultrafast magnetic dynamics, offering significant potential for next-generation spintronics [13–19].

Similar to electrons, magnons—the quanta of collective spin excitations in altermagnets—exhibit similar non-relativistic band splitting behavior [20–25]. Calculations based on linear spin wave theory (LSWT) demonstrate that the alternating isotropic spin exchange (ISE), governed by the combined spin and crystal symmetries in altermagnets, gives rise to the chiral magnon band splitting [20–22, 25, 26]. Extensive efforts have been devoted to exploring possible altermagnetic magnon band structures, but recent experimental observations show that the detected band splitting is extremely weak, displaying a pronounced deviation from theoretical predictions [27]. This discrepancy likely originates from the fact that the conventional Heisenberg model within LSWT fails to account for SOC effects [28–30]. More importantly, the influence of magnon–magnon interactions on spin exci-

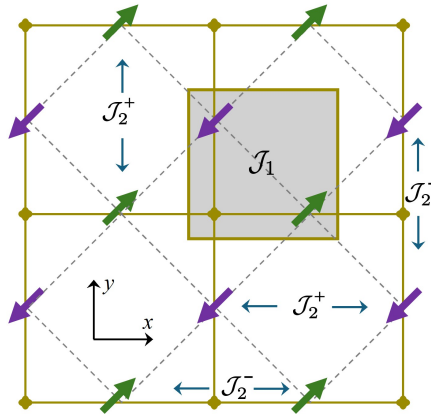


FIG. 1. The illustration of the the d -wave altermagnet on the square lattice. 2NN spin exchanges exhibit the d -wave behavior ($J_2^+ \neq J_2^-$) due to the breaking $\mathcal{PT}\tau$ symmetry between opposite-spin sublattices.

tations in altermagnets at a finite temperature remains largely unexplored.

In this work, based on renormalized spin-wave theory (RSWT), we demonstrate that in d -wave altermagnets, long-range anisotropic spin exchange (ASE), though suppressed at zero temperature, can effectively induce altermagnetic splitting of magnons at finite temperatures. Importantly, the altermagnetic splitting originating from ASE competes with that arising from alternating isotropic spin exchange (ISE), significantly modifying the overall altermagnetic magnon band structure as temperature increases. Moreover, this competing mechanism is strongly correlated with spin fluctuations, and can even reverse the sign of spin currents driven by the band splitting.

General spin model. In this work, we consider a mono-

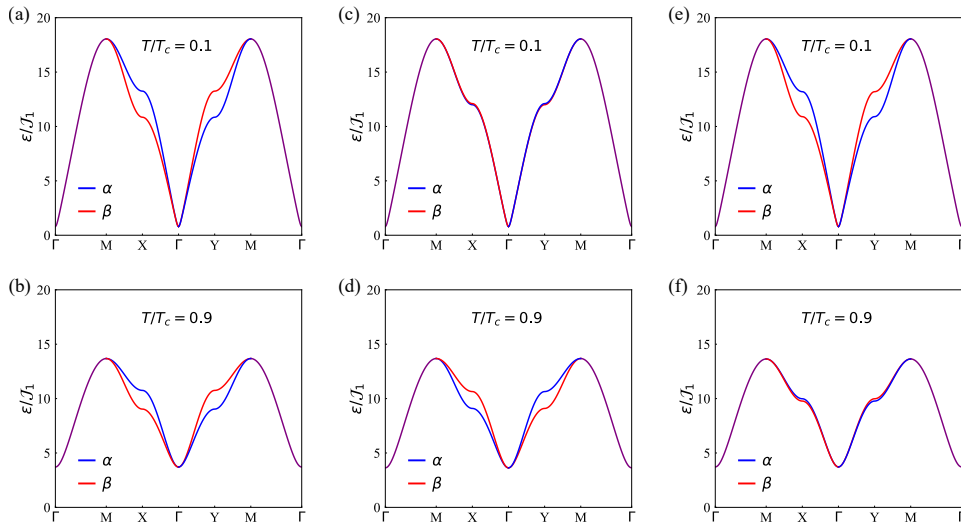


FIG. 2. Magnon bands of the monolayer d -wave altermagnet at different temperatures. (a)(b) With only ISE: $\Delta_J/J_1 = 0.2$. (c)(d) With only ASE: $J_{2z}/J_1 = 0.6$. (e)(f) With both ISE: $\Delta_J/J_1 = 0.2$ and ASE: $J_{2z}/J_1 = 0.6$.

layer d -wave square altermagnet, as illustrated in Fig. 1. The minimal spin model is given by

$$\hat{\mathcal{H}} = \hat{\mathcal{H}}_i + \hat{\mathcal{H}}_a + \hat{\mathcal{H}}_s, \quad (1)$$

where $\hat{\mathcal{H}}_i$ includes nearest-neighbor (NN) and second-nearest-neighbor (2NN) ISE, $\hat{\mathcal{H}}_a$ corresponds to 2NN ASE, and $\hat{\mathcal{H}}_s$ describes the magnetic anisotropy which aligns the spins along the z -axis. In addition, for simplicity, we restrict our analysis to cases where the spin angular momentum $\langle \mathcal{S}_z \rangle$ is conserved.

The first part of the spin Hamiltonian, $\hat{\mathcal{H}}_i$, can be written as

$$\begin{aligned} \hat{\mathcal{H}}_i = & J_1 \sum_{\langle i,j \rangle} \mathbf{S}_{i,\uparrow} \cdot \mathbf{S}_{j,\downarrow} \\ & + J_2^+ \sum_{\langle i,j \rangle'_x} \mathbf{S}_{i,\uparrow} \cdot \mathbf{S}_{j,\uparrow} + J_2^- \sum_{\langle i,j \rangle'_y} \mathbf{S}_{i,\uparrow} \cdot \mathbf{S}_{j,\uparrow} \quad (2) \\ & + J_2^- \sum_{\langle i,j \rangle'_x} \mathbf{S}_{i,\downarrow} \cdot \mathbf{S}_{j,\downarrow} + J_2^+ \sum_{\langle i,j \rangle'_y} \mathbf{S}_{i,\downarrow} \cdot \mathbf{S}_{j,\downarrow}, \end{aligned}$$

where the first term corresponds to NN ISE, and the other terms describe 2NN ISE. To maintain the collinear spin order, we impose that $J_1 > 0$ and $J_2 = \frac{J_2^+ + J_2^-}{2} < 0$. In monolayer d -wave altermagnets, the lattice symmetry naturally gives rise to a nonzero d -wave $\Delta_J = -\frac{J_2^+ - J_2^-}{2}$. $\hat{\mathcal{H}}_s$ represents the easy-axis single-ion anisotropy (SIA), described as $\hat{\mathcal{H}}_s = \mathcal{K} \sum_i (\mathcal{S}_i^z)^2$ with $\mathcal{K} < 0$. In the following discussion, we assume that $S = 3/2$, $J_2 = -J_1$, $\mathcal{K} = -0.01 J_1$.

Since $\langle \mathcal{S}_z \rangle$ is conserved and Dzyaloshinskii-Moriya Interaction (DMI) [31, 32] is forbidden, 2NN ASE contains only diagonal exchange terms J_2^{xx} , J_2^{yy} and J_2^{zz} [33]. In addition, the terms J_2^{xx} , J_2^{yy} could be incorporated into

the 2NN ISE term, allowing the ASE to be simplified as $J_2^{zz} S_i^z S_j^z$ [33]. Therefore, in d -wave altermagnetic square lattice, $\hat{\mathcal{H}}_a$ is given as

$$\begin{aligned} \hat{\mathcal{H}}_a = & J_{2z}^+ \sum_{\langle i,j \rangle'_x} S_{i,\uparrow}^z \cdot S_{j,\uparrow}^z + J_{2z}^- \sum_{\langle i,j \rangle'_y} S_{i,\uparrow}^z \cdot S_{j,\uparrow}^z \\ & + J_{2z}^- \sum_{\langle i,j \rangle'_x} S_{i,\downarrow}^z \cdot S_{j,\downarrow}^z + J_{2z}^+ \sum_{\langle i,j \rangle'_y} S_{i,\downarrow}^z \cdot S_{j,\downarrow}^z, \end{aligned} \quad (3)$$

Finally, to preserve the stability of the magnetic ground state, we assume that $J_{2z}^+ = -J_{2z}^- = J_{2z}$.

Spin wave theory. Next, we investigate the magnons of Eq. (1) based on the spin wave theory. Relying on a magnetically ordered classical ground state, we proceed with a Holstein-Primakoff (HP) transformation [34]

$$\begin{cases} S_{i,\uparrow}^z = +S - a_i^\dagger a_i (\hat{n}_i^a) \\ S_{i,\uparrow}^+ = \sqrt{2S - a_i^\dagger a_i} a_i \approx \sqrt{2S} a_i - \frac{a_i^\dagger a_i a_i}{\sqrt{8S}} \\ S_{i,\uparrow}^- = a_i^\dagger \sqrt{2S - a_i^\dagger a_i} \approx \sqrt{2S} a_i^\dagger - \frac{a_i^\dagger a_i^\dagger a_i}{\sqrt{8S}} \\ S_{j,\downarrow}^z = -S + b_j^\dagger b_j (\hat{n}_j^b) \\ S_{j,\downarrow}^+ = b_j^\dagger \sqrt{2S - b_j^\dagger b_j} \approx \sqrt{2S} b_j^\dagger - \frac{b_j^\dagger b_j^\dagger b_j}{\sqrt{8S}} \\ S_{j,\downarrow}^- = \sqrt{2S - b_j^\dagger b_j} b_j \approx \sqrt{2S} b_j - \frac{b_j^\dagger b_j b_j}{\sqrt{8S}} \end{cases} \quad (4)$$

At low temperatures ($T \ll \mathcal{J}$), the perturbations about the classical ground state is very small ($\langle \hat{n}_{i,j} \rangle \ll S$) [34–36]. Therefore, for a low-temperature effective model, the higher-order interactions can be neglected. We retain only the ground-state energy and the quadratic terms

in the bosonic operators, which together define as the first-order magnon Hamiltonian. Notably, the quadratic bosonic terms arising from the \mathcal{J}_{2z} spin exchanges does not appear in the first-order Hamiltonian, indicating that 2NN ASE makes no contribution to the LSWT model.

We then employ Fourier transformation,

$$a_{\mathbf{k}} = \frac{1}{\sqrt{N}} \sum_i a_i e^{+i\mathbf{k} \cdot \mathbf{R}_i}, \quad b_{\bar{\mathbf{k}}} = \frac{1}{\sqrt{N}} \sum_j b_j e^{-i\mathbf{k} \cdot \mathbf{R}_i} \quad (5)$$

where $\bar{\mathbf{k}}$ denotes magnons carrying momentum $-\mathbf{k}$. The first-order Hamiltonian can be expressed in the spinor basis $\psi_{\mathbf{k}}^{\dagger} = (a_{\mathbf{k}}^{\dagger}, b_{\bar{\mathbf{k}}}^{\dagger})$ as $\hat{\mathcal{H}}_1 = \sum_{\mathbf{k}} \psi_{\mathbf{k}}^{\dagger} \hat{\mathcal{H}}_{1\mathbf{k}} \psi_{\mathbf{k}}$, with details shown in the supplemental material (SM) [37]. Neglecting the zero-point energy, $\hat{\mathcal{H}}_{1\mathbf{k}}$ reads as

$$\frac{\hat{\mathcal{H}}_{1\mathbf{k}}}{S} = \lambda I + \begin{pmatrix} -\Delta_{\mathcal{J}} f_d & \mathcal{J}_1 f_{\times} \\ \mathcal{J}_1 f_{\times} & +\Delta_{\mathcal{J}} f_d \end{pmatrix}, \quad (6)$$

where $\lambda = 4\mathcal{J}_1 - 2\mathcal{K} + \mathcal{J}_2 f_s$ and the form factors $f_{\times}^{\mathbf{k}} = 4 \cos \frac{k_x}{2} \cos \frac{k_y}{2}$, $f_{x,y}^{\mathbf{k}} = 2 \cos k_{x,y} - 2$, $f_{s,d}^{\mathbf{k}} = f_x^{\mathbf{k}} \pm f_y^{\mathbf{k}}$. Using Bogoliubov transformations [38, 39], we can derive the analytical eigenvalues of Eq. (6), expressed as

$$\frac{\mathcal{E}_{\mathbf{k}}^{\alpha,\beta}}{S} = \sqrt{(4\mathcal{J}_1 + \mathcal{J}_2 f_s - 2\mathcal{K})^2 - (\mathcal{J}_1 f_{\times})^2} \mp \Delta_{\mathcal{J}} f_d. \quad (7)$$

It clearly shows that the emergence of $\mp \Delta_{\mathcal{J}}$ lifts the band degeneracy.

As shown in Fig 2.(a), the α and β modes are degenerate along the Γ -M and M- Γ paths because $|k_x| = |k_y|$, but as $\Delta_{\mathcal{J}} > 0$, the energy of the α mode is higher along the M-X- Γ path or near the X point as $|k_x| > |k_y|$ while the energy of the β mode is higher along the Γ -Y-M path or near the Y point as $|k_x| < |k_y|$. The magnon band splitting between α and β modes reaches its maximum at the X and Y points, defined as $\Delta_{\mathcal{E}} = \frac{\mathcal{E}_X^{\alpha} - \mathcal{E}_X^{\beta}}{2} = \frac{\mathcal{E}_Y^{\beta} - \mathcal{E}_Y^{\alpha}}{2}$. Here, $\Delta_{\mathcal{E}}$ is referred to as the band gap of altermagnetic magnons. To generalize, we introduce the ratio of this gap to the total bandwidth, $\phi = \frac{\mathcal{E}_X^{\alpha} - \mathcal{E}_X^{\beta}}{\mathcal{E}_+ - \mathcal{E}_-} = \frac{\mathcal{E}_Y^{\beta} - \mathcal{E}_Y^{\alpha}}{\mathcal{E}_+ - \mathcal{E}_-}$, which serves as the altermagnetic order parameter.

Many body effects. At the high temperature regime ($T \sim \mathcal{J}$), the magnon-magnon interactions cannot be neglected [30, 35, 40]. We extend the above spin Hamiltonian to include terms quartic in the bosonic operators, defined as the second order Hamiltonian $\hat{\mathcal{H}}_2$. Under the condition of momentum conservation, $\mathbf{k}_1 + \mathbf{k}_2 = \mathbf{k}_3 + \mathbf{k}_4$, the second order magnon Hamiltonian in \mathbf{k} space can be

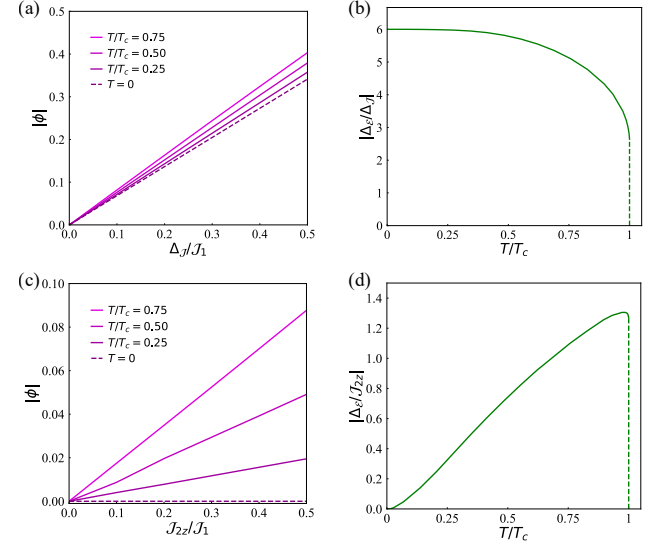


FIG. 3. Altermagnetic splitting of the d -wave altermagnet. (a)(c) Linear dependence of the order parameter ϕ on (a) ISE ($\Delta_{\mathcal{J}}/\mathcal{J}_1$) and (c) ASE ($\mathcal{J}_{2z}/\mathcal{J}_1$) at a given temperature. (b)(d) Dependence of the linear coefficients for (b) ISE ($\Delta_{\mathcal{E}}/\Delta_{\mathcal{J}}$) and (d) ASE ($\Delta_{\mathcal{E}}/\mathcal{J}_{2z}$) on temperature T .

expressed as

$$\begin{aligned} \hat{\mathcal{H}}_{2k} = & \frac{1}{N} \sum_{\{\mathbf{k}\}} -\mathcal{J}_1 f_{\times}^{\mathbf{q}'} a_{\mathbf{k}_1}^{\dagger} b_{\bar{\mathbf{k}}_3}^{\dagger} b_{\bar{\mathbf{k}}_2} a_{\mathbf{k}_4} \\ & + \frac{1}{4} \mathcal{J}_1 f_{\times}^{\mathbf{k}_1} b_{\bar{\mathbf{k}}_1}^{\dagger} a_{\mathbf{k}_2}^{\dagger} a_{\mathbf{k}_3} a_{\mathbf{k}_4} + \text{H.c.} \\ & + \frac{1}{4} \mathcal{J}_1 f_{\times}^{\mathbf{k}_4} b_{\bar{\mathbf{k}}_1}^{\dagger} b_{\bar{\mathbf{k}}_2}^{\dagger} b_{\bar{\mathbf{k}}_3} a_{\mathbf{k}_4}^{\dagger} + \text{H.c.} \\ & + (\mathcal{M}_{\{\mathbf{k}\}}^a + \mathcal{K}) a_{\mathbf{k}_1}^{\dagger} a_{\mathbf{k}_2}^{\dagger} a_{\mathbf{k}_3} a_{\mathbf{k}_4} \\ & + (\mathcal{M}_{\{\mathbf{k}\}}^b + \mathcal{K}) b_{\bar{\mathbf{k}}_1}^{\dagger} b_{\bar{\mathbf{k}}_2}^{\dagger} b_{\bar{\mathbf{k}}_3} b_{\bar{\mathbf{k}}_4}, \end{aligned} \quad (8)$$

where $\mathbf{q}' = \mathbf{k}_1 - \mathbf{k}_4$, and the coefficient $\mathcal{M}_{\{\mathbf{k}\}}$ stems from 2NN spin exchanges, especially 2NN ASE, and is expressed as

$$\begin{aligned} \mathcal{M}_{\{\mathbf{k}\}}^{a,b} = & \pm \left(\mathcal{J}_{2z} f_d^{\mathbf{q}} - \frac{\Delta_{\mathcal{J}}}{2} [2f_d^{\mathbf{q}} - f_d^{\mathbf{k}_1} - f_d^{\mathbf{k}_4}] \right) \\ & + \frac{\mathcal{J}_2}{2} [2f_s^{\mathbf{q}} - f_s^{\mathbf{k}_1} - f_s^{\mathbf{k}_4}], \end{aligned} \quad (9)$$

where $\mathbf{q} = \mathbf{k}_1 - \mathbf{k}_3 = \mathbf{k}_4 - \mathbf{k}_2$.

Next, we employ the Hartree-Fock (HF) approximation to deal with the magnon-magnon interactions. The HF approximation contracts the four-point interaction into the a sum of quadratic terms weighted by two-point correlation functions $\hat{C}_{\mathbf{k}}$ (for the formula of $\hat{C}_{\mathbf{k}}$ see the SM [37]). For instance, the first term of Eq. (8) could be

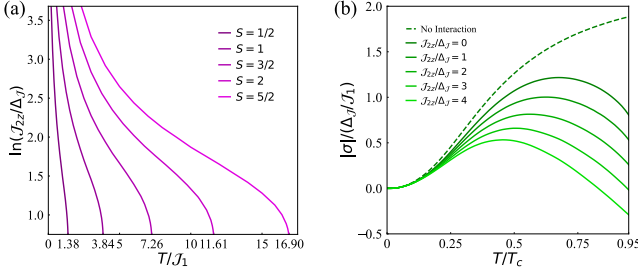


FIG. 4. (a) The dependence of the ISE/ASE ratio (J_{2z}/Δ_J) at which the altermagnetic gap vanishes completely on temperature T and spin number S . (b) The dependence of thermal spin conductivity σ on ratio J_{2z}/Δ_J and temperature T .

approximated as [41–43]

$$\delta_{\mathbf{k}_1+\mathbf{k}_2=\mathbf{k}_3+\mathbf{k}_4} a_{\mathbf{k}_1}^\dagger b_{\bar{\mathbf{k}}_3}^\dagger b_{\bar{\mathbf{k}}_2} a_{\mathbf{k}_4} \approx \\ + \delta_{\mathbf{k}_1=\mathbf{k}_3, \mathbf{k}_2=\mathbf{k}_4} \left[\langle a_{\mathbf{k}_1}^\dagger b_{\bar{\mathbf{k}}_3}^\dagger \rangle b_{\bar{\mathbf{k}}_2} a_{\mathbf{k}_4} + \langle b_{\bar{\mathbf{k}}_2} a_{\mathbf{k}_4} \rangle a_{\mathbf{k}_1}^\dagger b_{\bar{\mathbf{k}}_3}^\dagger \right] \\ + \delta_{\mathbf{k}_1=\mathbf{k}_4, \mathbf{k}_2=\mathbf{k}_3} \left[\langle a_{\mathbf{k}_1}^\dagger a_{\mathbf{k}_4} \rangle b_{\bar{\mathbf{k}}_3}^\dagger b_{\bar{\mathbf{k}}_2} + \langle b_{\bar{\mathbf{k}}_3}^\dagger b_{\bar{\mathbf{k}}_2} \rangle a_{\mathbf{k}_1}^\dagger a_{\mathbf{k}_4} \right]. \quad (10)$$

While the other terms could be approximated in a similar manner (for the details see the SM [37]). Specifically, the 2NN ASE term after the HF approximation can be expressed as

$$\hat{\mathcal{H}}_{2,\text{HF}}^a = \frac{1}{N} \sum_{\mathbf{k}, \mathbf{k}'} 2J_{2z} f_d^{\mathbf{k}'-\mathbf{k}} \left(\langle \hat{n}_{\mathbf{k}'}^a \rangle \hat{n}_{\mathbf{k}}^a - \langle \hat{n}_{\mathbf{k}'}^b \rangle \hat{n}_{\mathbf{k}}^b \right). \quad (11)$$

As a result, the overall effective Hamiltonian can be obtained by adding $\hat{\mathcal{H}}_{2,\text{HF}}$ to $\hat{\mathcal{H}}_1$, which only includes quadratic terms while effectively capturing the magnon-magnon interactions.

Based on the HF approximation, we calculate the renormalized magnon bands at finite temperatures. When only considering 2NN ISE, as shown in Figs. 2(a) and (b), increasing the temperature mainly modifies the shape of the magnon bands, while the altermagnetic splitting becomes slightly weaker, as 2NN ISE affects the energy of X/Y magnons directly and does not rely on other magnons. In contrast, when only including 2NN ASE, as shown in Figs. 2(c) and (d), the increase in temperature has a pronounced effect on the altermagnetic splitting. This is because that, as inferred from Eq.(11), ASE affects the bands by coupling the X/Y magnons with the Γ magnons and therefore strongly depends on the magnon population at the Γ point. For $J_{2z} > 0$, for the α band, ASE couples the X and Γ magnons attractively and the Y and Γ magnons repulsively, while for the β band, ASE couples the X and Γ magnons repulsively and the Y and Γ magnons attractively. Since the sign of the altermagnetic splitting induced by 2NN ASE is opposite to that caused by 2NN ISE, the altermagnetic splitting Δ_ε almost disappears at high temperature [see Fig. 2(f)] when

ISE and ASE share same sign. Interestingly, when J_{2z} and Δ_J have opposite signs, ASE conversely widens the altermagnetic splitting.

The temperature dependence of the order parameter ϕ and altermagnetic splitting Δ_ε are shown in Fig. 3. For a given temperature, ϕ exhibits a positive linear dependence on ISE. The linear coefficient $\Delta_\varepsilon/\Delta_J$ varies with T but changes slowly, indicating that ISE plays an important role across the entire temperature range. In contrast, as shown in Figs. 3(c) and (d), order parameter ϕ also exhibits a linear dependence on ASE, with the linear coefficient $\Delta_\varepsilon/J_{2z}$ varying almost linearly and positively with T . Therefore, the contribution of ASE becomes more significant at high temperatures.

Given that magnon-magnon interactions is related to the spin number S , it's essential to examine how the above competitive mechanism depends on S . As shown in Fig. 4(a), we determine the ratio between J_{2z} and Δ_J required for the altermagnetic gap to vanish at different S . For systems with only a small S , larger spin fluctuations lead to the closure of the altermagnetic gap at low temperature and a small ratio of J_{2z}/Δ_J . In contrast, in altermagnets with large S , the altermagnetic gap remains robust even at high temperature. This result provides important theoretical guidance for experimentally searching for robust altermagnetic magnons.

Spin currents. The altermagnetic chiral splitting of magnons leads to a spin current driven by the temperature gradient [21, 36, 44–47], known as the spin Seebeck effect. Given that spin conductivity is related to the splitting strength, the above competing mechanism between ASE and ISE has a significant impact on it. The thermal spin conductivity tensor σ_{mn} is defined by $\langle \mathbf{j}^z \rangle_m = -\sigma_{mn}(\nabla T)_n$, where $\langle \mathbf{j}^z \rangle$ is the spin current density and ∇T is the temperature gradient. Based on the Kubo formula, the spin conductivity σ_{mn} is given as

$$\sigma_{mn} = -\frac{\tau_0}{\hbar V T^2} \sum_{\mathbf{k}} \left(\mathbf{v}_{\mathbf{k}}^\alpha \right)_m \left(\mathbf{v}_{\mathbf{k}}^\alpha \right)_n \mathcal{E}_{\mathbf{k}}^\alpha \frac{e^{\mathcal{E}_{\mathbf{k}}^\alpha/T}}{\left(e^{\mathcal{E}_{\mathbf{k}}^\alpha/T} - 1 \right)^2} \\ + \frac{\tau_0}{\hbar V T^2} \sum_{\mathbf{k}} \left(\mathbf{v}_{\mathbf{k}}^\beta \right)_m \left(\mathbf{v}_{\mathbf{k}}^\beta \right)_n \mathcal{E}_{\mathbf{k}}^\beta \frac{e^{\mathcal{E}_{\mathbf{k}}^\beta/T}}{\left(e^{\mathcal{E}_{\mathbf{k}}^\beta/T} - 1 \right)^2}, \quad (12)$$

where $\mathbf{v}_{\mathbf{k}}^{\alpha, \beta} = \partial \mathcal{E}_{\mathbf{k}}^{\alpha, \beta} / \hbar \partial \mathbf{k}$, τ_0 is the average magnon lifetime and V is the volume. Note that $\tau_0 = \hbar/J_1$ and

TABLE I. DFT-calculated parameters and HF-calculated altermagnetic gaps in d -wave altermagnets MF_2 in which $M = \text{Ni, Co, Mn}$. Here, ϕ_t refers to the ϕ at $t = T/T_c$.

MF_2	S	Δ_J	J_{2z}/Δ_J	$\phi_{0.01}$	$\phi_{0.5}$	$\phi_{0.99}$
NiF_2	1	0.21	0.97	0.143	0.139	0.116
CoF_2	3/2	0.11	0.19	0.075	0.082	0.092
MnF_2	5/2	0.05	0.99	0.034	0.033	0.026

$k_B = 1$ for simplicity. The thermal spin conductivity tensor exhibits d -wave behavior and could be simplified into a scalar $\sigma = +\sigma_{xx} = -\sigma_{yy}$ as $\sigma_{xy} = \sigma_{yx} = 0$.

The calculated temperature dependence of thermal spin conductivity σ is shown in Fig. 4(b). Since σ depends linearly on altermagnetic splitting [21, 44], it also exhibits a linear dependence on ISE at low temperatures, where magnon–magnon interactions are weak. As temperature increases, the magnon–magnon interactions is essential, the emergence of the \mathcal{J}_{2z} narrow the altermagnetic splitting. Therefore, the giant ratio of $\mathcal{J}_{2z}/\Delta_{\mathcal{J}}$ can flip the sign of σ at the high temperature regime. This intriguing result provides experimental guidance for detecting altermagnetic magnons in the 2D limit.

Discussion and summary. The above results can be easily generalized from the d -wave altermagnet to other f -wave, g -wave and i -wave altermagnets, as well as from 2D materials to 3D materials. As shown in Tab. I, we present the altermagnetic splitting of magnons in the d -wave altermagnets MF_2 ($M = \text{Ni, Co, Mn}$) at the finite temperatures [22, 27]. This highlights that the ratio of $\mathcal{J}_{2z}/\Delta_{\mathcal{J}}$ play a decisive role in the altermagnetic splitting. For instance, in both NiF_2 and MnF_2 , the large ratio of $\mathcal{J}_{2z}/\Delta_{\mathcal{J}}$ substantially suppresses the altermagnetic gap at high temperatures. In contrast, the relatively small ratio of $\mathcal{J}_{2z}/\Delta_{\mathcal{J}}$ ensures that the altermagnetic gap in CoF_2 remain robust even for high temperatures. This suggest that $\Delta_{\mathcal{J}}$, \mathcal{J}_{2z} and S collectively determine the strength and thermal stability of the altermagnetic magnon splitting.

Importantly, this competitive mechanism between 2NN ASE and ISE is manifested in the spin currents induced by the band splitting. When \mathcal{J}_{2z} and $\Delta_{\mathcal{J}}$ share the same sign, their altermagnetic splitting is opposite, and when ratio of $\mathcal{J}_{2z}/\Delta_{\mathcal{J}}$ is large, there is a reversal of the spin current at the high temperature regime. Conversely, when they have opposite signs, the competition turns into cooperation, thereby enhancing both the altermagnetic splitting and the thermal response of the spin current.

In summary, by developing RSWT, we provide an accurate description of the finite-temperature behavior of altermagnetic magnons. Our results show that the magnitude of altermagnetic magnons splitting is determined by the ratio of $\mathcal{J}_{2z}/\Delta_{\mathcal{J}}$ and spin fluctuations. These factors also influence the sign and magnitude of the spin current induced by the band splitting. Our findings provide a new picture for understanding altermagnetic magnons and provide theoretical guidance for the design of novel spintronics.

Acknowledgments. The authors thank Prof. Guoqing Chang, Prof. Zhijun Zhang and Dr. Zhanlong Zhang for helpful discussions. This work is supported by the USTC Fellowship (Grant No. U19582025) and Young Talent Support Plan” of Xi'an Jiaotong University.

Data availability. All data are available from the au-

thors upon reasonable request.

* jyni@xjtu.edu.cn

- [1] T. Jungwirth, X. Marti, P. Wadley, and J. Wunderlich, Antiferromagnetic spintronics, *Nat. Nanotechnol.* **11**, 231 (2016).
- [2] V. Baltz, A. Manchon, M. Tsoi, T. Moriyama, T. Ono, and Y. Tserkovnyak, Antiferromagnetic spintronics, *Rev. Mod. Phys.* **90**, 015005 (2018).
- [3] L. Šmejkal, J. Sinova, and T. Jungwirth, Emerging research landscape of altermagnetism, *Phys. Rev. X* **12**, 040501 (2022).
- [4] L. Šmejkal, J. Sinova, and T. Jungwirth, Beyond conventional ferromagnetism and antiferromagnetism: A phase with nonrelativistic spin and crystal rotation symmetry, *Phys. Rev. X* **12**, 031042 (2022).
- [5] L. Šmejkal, R. González-Hernández, T. Jungwirth, and J. Sinova, Crystal time-reversal symmetry breaking and spontaneous Hall effect in collinear antiferromagnets, *Sci. Adv.* **6**, eaaz8809 (2020).
- [6] I. I. Mazin, K. Koepernik, M. D. Johannes, R. González-Hernández, and L. Šmejkal, Prediction of unconventional magnetism in doped FeSb_2 , *Proc. Nati. Acad. Sci.* **118**, e2108924118 (2021).
- [7] L. Bai, W. Feng, S. Liu, L. Šmejkal, Y. Mokrousov, and Y. Yao, Altermagnetism: Exploring new frontiers in magnetism and spintronics, *Adv. Funct. Mater.* **34**, 2409327 (2024).
- [8] Z. Zhou, X. Cheng, M. Hu, R. Chu, H. Bai, L. Han, J. Liu, F. Pan, and C. Song, Manipulation of the altermagnetic order in CrSb via crystal symmetry, *Nature* **638**, 645 (2025).
- [9] Y. Zhang, H. Bai, J. Dai, L. Han, C. Chen, S. Liang, Y. Cao, Y. Zhang, Q. Wang, W. Zhu, *et al.*, Electrical manipulation of spin splitting torque in altermagnetic RuO_2 , *Nat. Commun.* **16**, 5646 (2025).
- [10] X. Duan, J. Zhang, Z. Zhu, Y. Liu, Z. Zhang, I. Žutić, and T. Zhou, Antiferroelectric altermagnets: Antiferroelectricity alters magnets, *Phys. Rev. Lett.* **134**, 106801 (2025).
- [11] C. Song, H. Bai, Z. Zhou, L. Han, H. Reichlova, J. H. Dil, J. Liu, X. Chen, and F. Pan, Altermagnets as a new class of functional materials, *Nat. Rev. Mater.* **1** (2025).
- [12] P. Liu, J. Li, J. Han, X. Wan, and Q. Liu, Spin-group symmetry in magnetic materials with negligible spin-orbit coupling, *Phys. Rev. X* **12**, 021016 (2022).
- [13] R. He, D. Wang, N. Luo, J. Zeng, K.-Q. Chen, and L.-M. Tang, Nonrelativistic spin-momentum coupling in antiferromagnetic twisted bilayers, *Phys. Rev. Lett.* **130**, 046401 (2023).
- [14] X. Chen, J. Ren, Y. Zhu, Y. Yu, A. Zhang, P. Liu, J. Li, Y. Liu, C. Li, and Q. Liu, Enumeration and representation theory of spin space groups, *Phys. Rev. X* **14**, 031038 (2024).
- [15] Y. Jiang, Z. Song, T. Zhu, Z. Fang, H. Weng, Z.-X. Liu, J. Yang, and C. Fang, Enumeration of spin-space groups: Toward a complete description of symmetries of magnetic orders, *Phys. Rev. X* **14**, 031039 (2024).
- [16] Z. Xiao, J. Zhao, Y. Li, R. Shindou, and Z.-D. Song, Spin space groups: Full classification and applications, *Phys.*

Rev. X **14**, 031037 (2024).

[17] Y. Liu, J. Yu, and C.-C. Liu, Twisted magnetic van der Waals bilayers: An ideal platform for altermagnetism, *Phys. Rev. Lett.* **133**, 206702 (2024).

[18] P. Das, V. Leeb, J. Knolle, and M. Knap, Realizing altermagnetism in Fermi-Hubbard models with ultracold atoms, *Phys. Rev. Lett.* **132**, 263402 (2024).

[19] V. Leeb, A. Mook, L. Šmejkal, and J. Knolle, Spontaneous formation of altermagnetism from orbital ordering, *Phys. Rev. Lett.* **132**, 236701 (2024).

[20] L. Šmejkal, A. Marmodoro, K.-H. Ahn, R. González-Hernández, I. Turek, S. Mankovsky, H. Ebert, S. W. D’Souza, O. Šipr, J. Sinova, *et al.*, Chiral magnons in altermagnetic RuO₂, *Phys. Rev. Lett.* **131**, 256703 (2023).

[21] Q. Cui, B. Zeng, P. Cui, T. Yu, and H. Yang, Efficient spin Seebeck and spin Nernst effects of magnons in altermagnets, *Phys. Rev. B* **108**, L180401 (2023).

[22] R. Hoyer, R. Jaeschke-Ubiergo, K.-H. Ahn, L. Šmejkal, and A. Mook, Spontaneous crystal thermal Hall effect in insulating altermagnets, *Phys. Rev. B* **111**, L020412 (2025).

[23] Z. Liu, M. Ozeki, S. Asai, S. Itoh, and T. Masuda, Chiral split magnon in altermagnetic MnTe, *Phys. Rev. Lett.* **133**, 156702 (2024).

[24] M. Alaei, P. Sobieszczyk, A. Ptak, N. Rezaei, A. R. Oganov, and A. Qaiumzadeh, Origin of A-type antiferromagnetism and chiral split magnons in altermagnetic α -MnTe, *Phys. Rev. B* **111**, 104416 (2025).

[25] Q. Sun, J. Guo, D. Wang, D. L. Abernathy, W. Tian, and C. Li, Observation of chiral magnon band splitting in altermagnetic hematite, *Phys. Rev. Lett.* **135**, 186703 (2025).

[26] R. Hoyer, P. P. Stavropoulos, A. Razpopov, R. Valentí, L. Šmejkal, and A. Mook, Altermagnetic splitting of magnons in hematite α -Fe₂O₃, *Phys. Rev. B* **112**, 064425 (2025).

[27] V. C. Morano, Z. Maesen, S. E. Nikitin, J. Lass, D. G. Mazzone, and O. Zaharko, Absence of altermagnetic magnon band splitting in MnF₂, *Phys. Rev. Lett.* **134**, 226702 (2025).

[28] J. L. Lado and J. Fernández-Rossier, On the origin of magnetic anisotropy in two dimensional CrI₃, *2D Materials* **4**, 035002 (2017).

[29] D. Šabani, C. Bacaksiz, and M. V. Milošević, Beyond orbitally resolved magnetic exchange in CrI₃ and NiI₂, *Phys. Rev. Lett.* **135**, 036704 (2025).

[30] A. Mook, K. Plekhanov, J. Klinovaja, and D. Loss, Interaction-stabilized topological magnon insulator in ferromagnets, *Phys. Rev. X* **11**, 021061 (2021).

[31] I. Dzyaloshinsky, A thermodynamic theory of “weak” ferromagnetism of antiferromagnetics, *J. Phys. Chem. Solids* **4**, 241 (1958).

[32] T. Moriya, Anisotropic superexchange interaction and weak ferromagnetism, *Phys. Rev.* **120**, 91 (1960).

[33] Since DMI interaction is forbidden due to the inversion symmetry, the 2NN ASE tensor is symmetric. The conservation of $\langle S_z \rangle$ is directly leads to easy-axis anisotropy, which requires that the off-diagonal elements vanish, $\mathcal{J}_2^{xz} = \mathcal{J}_2^{yz} = \mathcal{J}_2^{xy} = 0$, and in-plane diagonal elements be degenerate, $\mathcal{J}_2^{xx} = \mathcal{J}_2^{yy}$. Consequently, the 2NN ASE term can be further simplified as $\mathcal{J}_2^s(\mathbf{S}_i \cdot \mathbf{S}_j) + (\mathcal{J}_2^{zz} - \mathcal{J}_2^s)S_i^z S_j^z$, where $\mathcal{J}_2^s = \mathcal{J}_2^{xx} = \mathcal{J}_2^{yy}$.

[34] T. Holstein and H. Primakoff, Field dependence of the intrinsic domain magnetization of a ferromagnet, *Phys. Rev.* **58**, 1098 (1940).

[35] M. Zhitomirsky and A. Chernyshev, Colloquium: Spontaneous magnon decays, *Rev. Mod. Phys.* **85**, 219 (2013).

[36] J. Ni, Y. Jin, Q. Du, and G. Chang, Magnon nonlinear Hall effect in two-dimensional antiferromagnetic insulators, *Phys. Rev. B* **112**, 054424 (2025).

[37] See Supplemental Material at ... for more details about.

[38] N. N. Bogoljubov, V. V. Tolmachov, and D. Širkov, A new method in the theory of superconductivity, *Fortschr. Phys.* **6**, 605 (1958).

[39] J. Valatin, Comments on the theory of superconductivity, *Il Nuovo Cimento (1955-1965)* **7**, 843 (1958).

[40] K. Souriounis and A. Manchon, Impact of magnon interactions on transport in honeycomb antiferromagnets, *Phys. Rev. B* **110**, 054429 (2024).

[41] Z. Li, T. Cao, and S. G. Louie, Two-dimensional ferromagnetism in few-layer van der Waals crystals: Renormalized spin-wave theory and calculations, *J. Magn. Magn. Mater.* **463**, 28 (2018).

[42] V. V. Mkhitarian and L. Ke, Self-consistently renormalized spin-wave theory of layered ferromagnets on the honeycomb lattice, *Phys. Rev. B* **104**, 064435 (2021).

[43] B. Wei, J.-J. Zhu, Y. Song, and K. Chang, Renormalization of gapped magnon excitation in monolayer MnBi₂Te₄ by magnon-magnon interaction, *Phys. Rev. B* **104**, 174436 (2021).

[44] K. Wu, J. Dong, M. Zhu, F. Zheng, and J. Zhang, Magnon splitting and magnon spin transport in altermagnets, *Chin. Phys. Lett.* (2025).

[45] Y. Onose, T. Ideue, H. Katsura, Y. Shiomi, N. Nagaosa, and Y. Tokura, Observation of the magnon Hall effect, *Science* **329**, 297 (2010).

[46] R. Cheng, S. Okamoto, and D. Xiao, Spin Nernst effect of magnons in collinear antiferromagnets, *Phys. Rev. Lett.* **117**, 217202 (2016).

[47] V. A. Zyuzin and A. A. Kovalev, Magnon spin Nernst effect in antiferromagnets, *Phys. Rev. Lett.* **117**, 217203 (2016).